

Scaling invariance of the homoclinic tangle

L. Kuznetsov*

Lefschetz Center for Dynamical Systems, Brown University, Providence, Rhode Island

G. M. Zaslavsky†

Courant Institute of Mathematical Sciences, New York University, 251 Mercer Street, New York, New York 10012

(Received 15 April 2002; published 21 October 2002)

The structure of the homoclinic tangle of $1\frac{1}{2}$ degrees of freedom Hamiltonian systems in the neighborhood of the saddle point is invariant under discrete rescaling of the system's parameters. The rescaling constant is derived from the separatrix map and the Melnikov formula. Invariant manifolds for the periodically modulated Duffing oscillator are computed numerically to confirm this property. The scaling is related to the recently found invariance of the separatrix map under a discrete renormalization group. A possibility to extend the scaling invariance to different systems is demonstrated. The equivalency conditions under which two systems have the similarity of their chaotic layer structure near the saddle are derived. A numerical example shows a Duffing oscillator and a pendulum (acted on by different periodic perturbations) with the same structure of the tangle.

DOI: 10.1103/PhysRevE.66.046212

PACS number(s): 05.45.Ac, 05.45.Pq

I. INTRODUCTION

Hamiltonian systems with low number of degrees of freedom arise in a variety of physical applications, such as advection of passive particles in incompressible flows [1–7], geometry of magnetic field lines in tokamaks [8,9], electron motion in a lattice [10,11], celestial mechanics [12,13], etc. A generic property of such systems is the coexistence of chaotic and regular trajectories. The partition of the phase space into regular and chaotic components is nontrivial, and leads to peculiar statistical properties of the trajectories in the chaotic component [14–18]. For example, the variance of the particle ensemble grows superdiffusively, $\sigma^2 \sim t^\mu$, $\mu > 1$, the distribution of the Poincaré recurrences is non-Poissonian, etc. The mechanism responsible for the anomalous statistics is the stickiness of the trajectories to the boundaries between the chaotic and regular components. The boundary zone is stratified with partial barriers (cantori) and has an infinite set of islands of regular motion. Due to its (multi)fractal structure, the boundary zone acts as a particle trap: the distribution of exit times has long algebraic tails. The connection between the structure of the phase space and the transport properties was investigated theoretically and numerically in a number of works [3,15–17,19–25]. To achieve a comprehensive description of particle kinetics in the chaotic layer a knowledge of fractal properties of the boundary zone is necessary.

The transition from the regular, integrable dynamics to chaotic dynamics was studied extensively in the framework of $1\frac{1}{2}$ degrees of freedom near-integrable systems [8,26,27]. In such systems the Hamiltonian is given by a sum of a

time-independent part H_0 and a small time-periodic perturbation: $H = H_0(x, y) + \epsilon V(x, y, t)$, $\epsilon \ll 1$. For $\epsilon \neq 0$ and generic V , the separatrices of the unperturbed system are replaced by chaotic layers. As $\epsilon \rightarrow 0$ the width of the layer decreases, but it retains the full complexity of its structure. The width of the chaotic layer has different expressions depending on ϵ and the frequency of perturbation, and it can be evaluated using the separatrix map [8]. There were different improvements and generalizations of the separatrix map in Refs. [28,29].

It was found in Ref. [30] that the structure of the layer near the saddle-point changes periodically with $\ln \epsilon$. More specifically, the phase portraits in the saddle-point neighborhood are invariant under simultaneous rescaling of the canonical coordinates and the perturbation amplitude according to $\epsilon \rightarrow \lambda \epsilon$, $(x, p) \rightarrow \lambda^{1/2}(x, p)$, where λ is a constant depending on H_0 and V . The origin of this property was traced to the renormalization invariance of the corresponding separatrix map. This rescaling was found in a variety of systems [30–34] and its manifestation in a $\ln \epsilon$ -periodic oscillations of transport characteristics was observed numerically [33,34].

In this work, we further investigate the scaling invariance of the chaotic layer originating from the renormalization invariance of the separatrix map. Our results include the formulation of the scaling property in terms of the system's parameters and the effect of the rescaling on the invariant manifolds attendant to the saddle. We show that a similarity between the chaotic layer structures extends to systems with different H_0 and/or V , i.e., the layer structure possesses certain universality. We derive the equivalency conditions that have to be satisfied in order for the two systems to have the same layer structure near the saddle. As an example, we demonstrate that for any (periodically perturbed) Duffing oscillator there is a (periodically perturbed) pendulum with the same layer structure.

The paper is organized as follows. In Sec. II we show how

*Electronic address: leonid@cfm.brown.edu;

URL: <http://www.cfm.brown.edu/people/leonid/webpage>

†Also at Department of Physics, New York University, New York, NY 10003, USA.

the formulation of the rescaling property in terms of system's parameters follows naturally from the expression for the Melnikov function. The Duffing oscillator is taken as an example; the rescaling of the homoclinic tangle is confirmed by numerical construction of the invariant manifolds. In Sec. III the connection to the corresponding invariance of the separatrix map is shown. In Sec. IV the case of two different systems is addressed.

II. MODULATED DUFFING OSCILLATOR

Consider a Duffing oscillator with periodically modulated frequency

$$H_\epsilon(p, x, t) = p^2/2 - x^2/2[1 + \epsilon \cos(\nu t + \phi_0)] + x^4/4a^2, \quad (1)$$

where ϵ and ν are the amplitude and the frequency of the modulation, and a is the parameter controlling the size of the unperturbed double-well potential. This system has an equilibrium saddle-point at zero: $x_s=0$, $p_s=0$. Stable and unstable manifolds W^s and W^u , associated with it are defined as sets of points with trajectories asymptotic to the saddle in forward and backward time, respectively [35]:

$$\begin{aligned} W^s &\equiv \{(x, p, t) | x(t_1; x, p, t) \rightarrow 0 \text{ as } t_1 \rightarrow \infty\}, \\ W^u &\equiv \{(x, p, t) | x(t_1; x, p, t) \rightarrow 0 \text{ as } t_1 \rightarrow -\infty\}, \end{aligned} \quad (2)$$

where $x(t_1; x, p, t)$ is a solution of the equations of motion with the initial condition $x(t) = x$, $p(t) = p$.

When $\epsilon = 0$, the energy $E \equiv H_0(p, x)$ is conserved, and the stable and unstable manifolds coincide along the separatrix curve $H_0(p, x) = 0$. There are two families of aperiodic separatrix solutions:

$$x_s^\sigma(t; \tau) = \sigma \frac{\sqrt{2}a}{\cosh(t - \tau)}, \quad (3)$$

$$p_s^\sigma(t; \tau) = -\sigma \frac{\sqrt{2}a \sinh(t - \tau)}{\cosh^2(t - \tau)}, \quad (4)$$

where σ is $+1$ for the right branch and -1 for the left one. The solutions are parametrized by τ , the time of the center of the pulse (maximum of $|x_s|$). The period of near separatrix trajectories (with $E \ll 1$) diverges as $E \rightarrow 0$ as

$$T(E) = \ln \frac{16a^2}{|E|}, \quad (5)$$

When $\epsilon \neq 0$, W^s and W^u intersect transversely and form a homoclinic tangle. For small ϵ the distance between them can be estimated by Melnikov formula [26,35]:

$$d(\tau) \approx \epsilon M(\tau) / |\nabla H_0|, \quad (6)$$

where the Melnikov integral is given by:

$$M(\tau) = \int_{-\infty}^{-\infty} p_s(t; \tau) x_s(t; \tau) \cos(\nu t + \phi_0) dt, \quad (7)$$

$$M(\tau) = M_d \sin(\nu \tau + \phi_0), \quad M_d = \frac{\pi \nu^2 a^2}{\sinh(\pi \nu / 2)}. \quad (8)$$

Zeros of the Melnikov function

$$t_n = \pi n / \nu, \quad x_n = \pm \sqrt{2}a / \cosh(\pi n / \nu), \quad n \in \mathbf{Z} \quad (9)$$

correspond to the primary intersection points of W^s and W^u .

The primary intersection points accumulate near the saddle, where $|n|$ is large and

$$x_n \approx p_n \approx \pm \sqrt{2}a e^{-\pi |n| / \nu}. \quad (10)$$

The change of the Hamiltonian parameter $a \rightarrow \lambda a$ changes the location of the primary intersections in the vicinity of the saddle unless we take

$$\lambda = \lambda_a^m = e^{-\pi m / \nu}, \quad m = \pm 1, \pm 2, \dots \quad (11)$$

when the intersections are mapped to each other:

$$x_n \rightarrow x_{n+m} \quad (n > 0), \quad x_n \rightarrow x_{n-m} \quad (n < 0). \quad (12)$$

In order to preserve the structure of the homoclinic tangle two other conditions have to be satisfied. First, the area of the lobes [the regions bounded by the pieces on W^s and W^u between two adjacent primary intersections, see, e.g., Ref. [35]] has to stay the same after the rescaling, and second, the manifold orientation at the intersection has to be preserved. All lobes have equal area

$$A_L = \left| \epsilon \int_{t_n}^{t_{n+1}} M(\tau) d\tau \right| = \epsilon M_d / \nu, \quad (13)$$

where M_d is defined in Eq. (8), and to keep it constant the perturbation amplitude has to be rescaled according to $|\epsilon| \rightarrow \lambda_a^{-2m} |\epsilon|$. To preserve the manifold orientation, the sign of ϵ has to be changed when m is odd, which leads to the following scaling:

$$a \rightarrow \lambda_a^m a, \quad \epsilon \rightarrow (-1)^m \lambda_a^{-2m} \epsilon. \quad (14)$$

Note, that changing the sign of ϵ is equivalent to the shift of the perturbation phase by π , $\phi_0 \rightarrow \phi_0 + \pi$.

It is not evident yet whether the secondary and higher-order intersections will be mapped to each other by the above scaling. In the following section we will show that the separatrix map that approximates the chaotic layer dynamics for small ϵ is invariant under the above rescaling, and, therefore, the structure of the homoclinic tangle near the saddle should be preserved.

Numerical examples corroborate this result. Left column in Fig. 1 shows the manifolds for the Duffing oscillator (1) for $\nu = 3\pi/2$, $\epsilon = \epsilon_0 = 0.1$, $a = a_0 = 1$. The rescaling constant for this frequency is $\lambda_a = \exp(\pi/\nu) = 1.947 \dots$. According to Eqs. (11), and (14), the same system with $\epsilon_1 = -\lambda_a^{-2} \epsilon_0 = -0.026 \dots$ and $a_1 = \lambda_a a_0 = 1.947 \dots$ will have the same structure of the manifolds. The right column of Fig. 1 shows the manifolds for these values of a and ϵ . The structure of the tangles around the saddle is remarkably similar (bottom

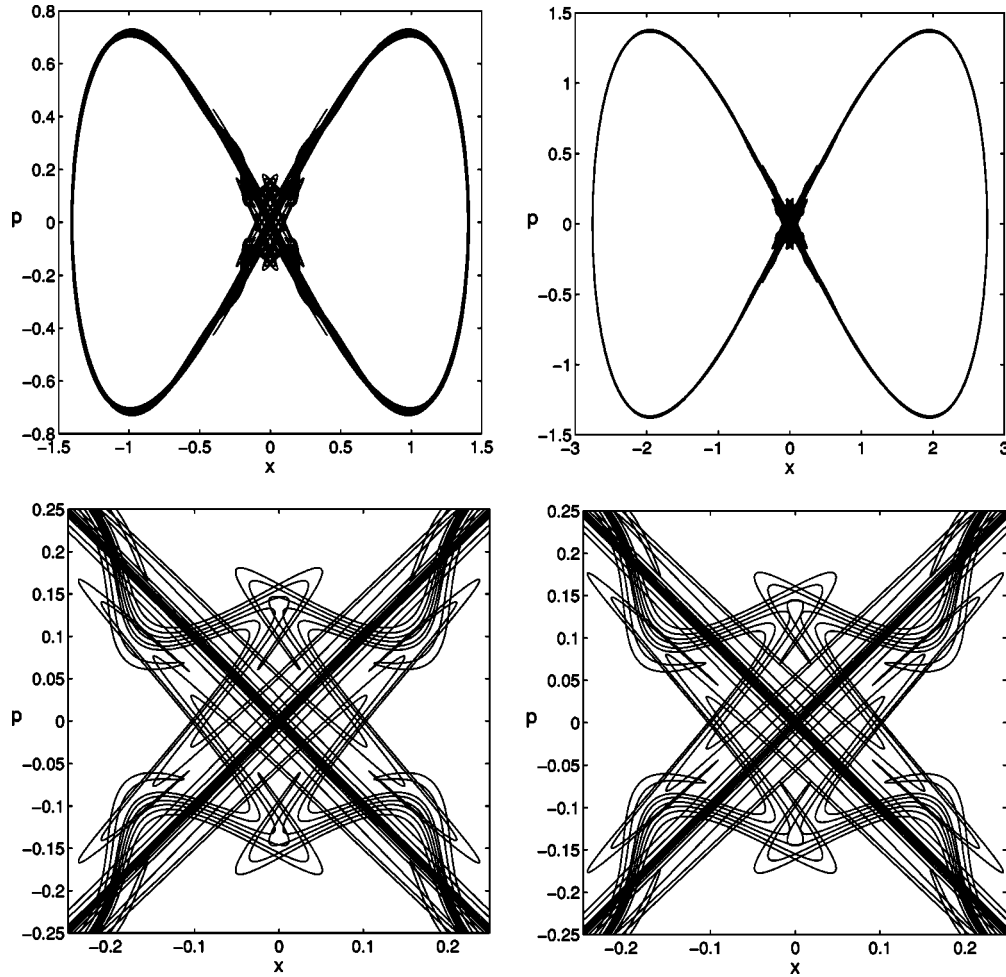


FIG. 1. Top row (pictures at different scale): Invariant manifolds for Duffing oscillator (1) with $\nu=3/2\pi$. Left column: $\epsilon_0=0.1$, $a_0=1$; right column: $\epsilon_1=0.027$, $a_1=1.947$. Bottom row (pictures at the same scale): Zoom of the saddle-point neighborhood.

row of Fig. 1). The difference between the two pictures is due to the relatively large perturbation amplitudes used: the width of the chaotic component near the saddle is of the same order of magnitude as the characteristic size of the potential well a . Although it is hard to discern it from the top row of Fig. 1, it is clear from Eq. (12) that the effect of the rescaling on the global structure of the tangle is the appearance of an extra primary intersection (and, therefore, an extra lobe).

The manifolds were computed via the straddling algorithm [36], the integration was carried out with a fifth-order symplectic scheme [37], with the time step $\Delta t=0.001$ and spatial resolution of the manifolds $\Delta x=0.01$. The choice of a high-precision integration scheme in combination with a very short time step was necessitated by a sensitive dependence of the near-saddle dynamics on numerical errors.

III. SEPARATRIX MAP AND THE ENERGY SCALE CONSTANT

A generic near-integrable $1\frac{1}{2}$ degrees of freedom Hamiltonian system

$$\dot{x} = \frac{\partial H_\epsilon}{\partial y}, \quad \dot{y} = -\frac{\partial H_\epsilon}{\partial x} \quad (15)$$

is defined by a Hamiltonian

$$H_\epsilon(x, y, t) = H_0(x, y) + \epsilon V(x, y, t) \quad (16)$$

that is given by the sum of an integrable part $H_0(x, y)$ and a time-periodic perturbation

$$V(x, y, t + 2\pi/\nu) = V(x, y, t) \quad (17)$$

with frequency ν and a small amplitude $\epsilon \ll 1$.

We assume that the unperturbed Hamiltonian H_0 has a saddle point (x_s, y_s) . A coordinate system can always be chosen in such a way that the saddle is at the origin, $x_s = y_s = 0$, and H_0 has the first terms of Taylor series expansion in the form

$$H_0(x, y) = E_s + y^2/2 - x^2/2 + o(x^2, y^2, xy). \quad (18)$$

In the absence of perturbation ($\epsilon=0$) the energy $E \equiv H_0(x, y)$ is a constant of motion, and the trajectories lie of the level curves $H_0(x, y) = \text{const}$.

The separatrix is the level curve passing through the saddle point. It self-intersects at the saddle, where it is tangent to the lines $x = \pm y$. In the following, we assume that there is no other fixed points on the separatrix. In that case it consists of two branches, each branch corresponds to a family of aperiodic homoclinic solutions $[x_s^\sigma(t - \tau), y_s^\sigma(t - \tau)]$. The sign variable $\sigma = \pm 1$ differentiates between the branches. These solutions have a solitonlike shape (τ corresponds to the soliton's center), their asymptotics follows from Eq. (18):

$$x_s^\sigma(t) \approx \sigma \exp(\pm t), \quad y_s^\sigma(t) \approx \pm \sigma \exp(\pm t), \quad t \rightarrow \mp \infty. \quad (19)$$

The construction of the separatrix map is based on generic properties of trajectories with $|E - E_s| \ll 1$. Such trajectory looks like a periodic sequence of localized pulses, separated by relatively long intervals when it stays in the neighborhood of the saddle. Depending on the sign of $E - E_s$, a trajectory may pass the saddle-point neighborhood once per period, in which case we will refer to it as a single passage trajectory, or twice per period, in which case we will call it a double passage one. The structure of H_0 determines which sign of $E - E_s$ corresponds to single passage trajectories, and which to double passage ones. In both cases the interval between the pulses diverges logarithmically when $E \rightarrow E_s$:

$$T \approx \ln(B/|E - E_s|), \quad E \rightarrow E_s, \quad (20)$$

where B is the *energy scale constant*. It is defined by the length of the separatrix loop and therefore depends on the specific form of the potential. Here we restrict our consideration to the symmetric case, where B is the same for both separatrix branches, however, the results can be generalized to the case when B depends on σ . The shape of each pulse is close to that of the separatrix solitons $[x^\sigma(t - \tau), y^\sigma(t - \tau)]$. A double passage trajectory consists of a series of alternating pulses with $\sigma = \pm 1$, a single passage one has pulses of the same shape.

When the perturbation is present, the energy is not conserved anymore, and the near-separatrix motion becomes chaotic. The trajectories still look like sequences of pulses, but the interval between them is not constant and there is no particular order in alternation between different branches, because the energy can change sign during the motion. The sequence of pulses can be described by three discrete variables: τ_n : time of the middle of the n th pulse, E_n : energy at the point of the nearest approach to the saddle between τ_{n-1} and τ_n , and σ_n : sign variable indicating which branch of the separatrix was followed by the n th pulse. Figure 2 illustrates the definition of these variables.

A map, approximating the dynamics of (τ, E, σ) was introduced in Ref. [8] [see, also, Refs. [27,38,39]] and is known as the *separatrix map*. It provides an efficient tool for the study of different properties of the near-separatrix dynamics: the width of the chaotic layer, the structure of resonant islands inside it, transport phenomena, etc. [40–42].

To construct the separatrix map, we need the equation for the evolution of the energy:

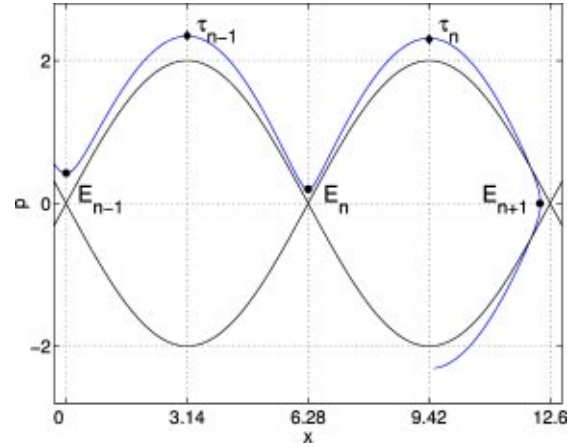


FIG. 2. Definition of the separatrix map variables.

$$\dot{E} = \epsilon [H_0, V], \quad (21)$$

where $[,]$ denotes the usual Poisson bracket. The change of the energy during one pulse is then

$$\Delta E(\tau_n, \sigma_n) = \epsilon \int_{\tau_n - T(E_n)/2}^{\tau_n + T(E_n)/2} [H_0, V] dt, \quad (22)$$

where $x(t)$ and $y(t)$ under the integral are taken along the trajectory. To evaluate the integral two approximations are made: $x(t)$ and $y(t)$ are replaced by $x_n^\sigma(t - \tau_n)$ and $y_n^\sigma(t - \tau_n)$, and integration limits are extended to $\pm \infty$ [see Refs. [38,43] for detail]. Then

$$\Delta E(\tau_n, \sigma_n) \approx \epsilon \int_{-\infty}^{\infty} [H_0, V] dt = \epsilon M(\tau_n, \sigma_n), \quad (23)$$

where $M(\tau_n, \sigma_n)$ is the Melnikov integral, which does not depend on E_n , and is periodic in τ_n :

$$M(\tau_n, \sigma_n) = M(\tau_n + 2\pi/\nu, \sigma_n). \quad (24)$$

The energy between the pulses is almost constant and equal to the midway energy E_{n+1} , therefore, the interval between the pulses can be approximated using Eq. (20) as

$$\tau_{n+1} - \tau_n = \ln(B/|E_{n+1} - E_s|). \quad (25)$$

The equation for σ_n depends on which sign of the $E - E_s$ corresponds to double passage trajectories. The trajectory switches separatrix branches at the saddle, $\sigma_{n+1} = -\sigma_n$, if E_{n+1} corresponds to a double passage trajectory, and stays on the same branch otherwise. Introducing the sgn constant $s = +1$ for the case when double passage trajectories have $E < E_s$ and $s = -1$ otherwise, we obtain

$$\sigma_{n+1} = s \sigma_n \operatorname{sgn}(E_{n+1} - E_s). \quad (26)$$

It is convenient to introduce new variables: an energy measured from the separatrix and the perturbation phase at the center of the n th pulse:

$$h_n \equiv E_n - E_s, \quad \phi_n \equiv \nu \tau_n, \quad \text{mod } 2\pi. \quad (27)$$

Now the separatrix map can be written as:

$$\begin{aligned} h_{n+1} &= h_n + \epsilon M(\phi_n, \sigma_n), \\ \phi_{n+1} &= \phi_n + \nu \ln B / |h_{n+1}|, \quad \text{mod } 2\pi, \\ \sigma_{n+1} &= s \sigma_n \operatorname{sgn}(h_{n+1}). \end{aligned} \quad (28)$$

If there is a parameter α in the Hamiltonian, i.e., $H_0 = H_0(x, p; \alpha)$, $V = V(x, p, t; \alpha)$, then the energy scale constant B and the Melnikov integral M will depend on this parameter. The invariance of the separatrix map with respect to the parameter rescaling can be formulated as follows.

Any change of Hamiltonian parameters $\alpha \rightarrow \alpha'$ resulting in the rescaling of B according to

$$B(\alpha) \rightarrow \lambda^m B(\alpha'), \quad m = \pm 1, \pm 2, \dots \quad (29)$$

together with the rescaling of the perturbation amplitude

$$\epsilon \rightarrow \epsilon M(\alpha') / M(\alpha) \quad (30)$$

leaves the separatrix map (28) invariant, if the rescaling constant is an integer power of

$$\lambda = \exp(2\pi/\nu). \quad (31)$$

Indeed, Eq. (30) preserves the product ϵM , so the first equation does not change, while Eq. (29) results in the appearance of an additional term $\nu m \ln \lambda$ in the second equation. With λ chosen according to Eq. (31), this term is zero, mod 2π , therefore the second equation is also preserved. The third equation is unaffected by Eqs. (29) and (30). The above invariance of the separatrix map is similar to the invariance with respect to the rescaling of ϵ and h by the same constant λ [given by Eq. (31)], which was obtained in Ref. [30].

The scaling (14) derived in Sec. II coincides with Eqs. (29) and (30) (with $\lambda = \lambda_\alpha^2$ due to $B \sim a^2$) except for the factor $(-1)^m$ in the formula for the perturbation amplitude ϵ . This difference is due to the nature of the separatrix map variables (h_n, τ_n) , which are taken at different points in time. The phase variable in Eq. (28) can be shifted in order to synchronize the two variables. The resulting equations, known as the shifted separatrix map [30], require the perturbation phase shift $m\pi$ in order to stay invariant under the rescaling [see, Refs. [30,32] for detail]. Such shift is equivalent to the factor $(-1)^m$ in the rescaling of the amplitude, i.e., the scaling Eq. (14) derived for the homoclinic coincides with the scaling for the corresponding shifted separatrix map.

IV. SCALING UNIVERSALITY

In this section, we will formulate the universality property of chaotic layer structure in near-integrable Hamiltonian systems with $1\frac{1}{2}$ degrees of freedom. Our main conjecture is that if separatrix maps, approximating two different systems are equivalent (i.e., can be made the same by an appropriate change of variables), then the phase portraits of these systems are similar (i.e., have the same topology and can be obtained from each other by the rescaling of the coordinates)

in the neighborhood of the saddles. We will list the conditions for this equivalency, and support it with numerical examples.

Consider two near-integrable Hamiltonian systems of the following form:

$$H^{(i)} = H_0^{(i)}(x, y) + \epsilon_i f_i(x, y) \sin \nu_i t, \quad i = 1, 2. \quad (32)$$

We assume, that both $H_0^{(1)}$ and $H_0^{(2)}$ have saddle points at zero, and their Taylor expansions at the saddle are

$$H_0^{(i)} = E_s^{(i)} + y^2/2 - \gamma_i^2 x^2/2 + o(x^2, y^2, xy), \quad i = 1, 2. \quad (33)$$

It follows that the interval between two velocity pulses of near separatrix trajectories diverges logarithmically in both systems as

$$T_i \approx \gamma_i^{-1} \ln \frac{B_i}{|E - E_s^{(i)}|}, \quad i = 1, 2 \quad (34)$$

provided there is no other saddles on the separatrices. The energy scale constants B_i depend on $H_0^{(i)}$ but not on $V^{(i)}$ (see, Sec. III). Separatrix map for each system can be written as ($i = 1, 2$):

$$\begin{aligned} E_{n+1}^{(i)} &= E_n^{(i)} + \epsilon_i M_i(\sigma_n^{(i)}) \sin \phi_n^{(i)}, \\ \phi_{n+1}^{(i)} &= \phi_n^{(i)} + (\nu_i / \gamma_i) \ln(B_i / |E_{n+1}^{(i)} - E_s^{(i)}|), \quad \text{mod } 2\pi, \\ \sigma_{n+1}^{(i)} &= s_i \sigma_n^{(i)} \operatorname{sgn}(E_{n+1}^{(i)} - E_s^{(i)}). \end{aligned} \quad (35)$$

Sign constant s_i is $s_i = 1$ if the double passage trajectories have $E < E_s$, and $s_i = -1$ otherwise.

Let us rescale the energy according to

$$h^{(i)} = s_i (E^{(i)} - E_s^{(i)}) / B_i. \quad (36)$$

The maps (35) can be rewritten as

$$\begin{aligned} h_{n+1}^{(i)} &= h_n^{(i)} + [s_i \epsilon_i M_i(\sigma_n^{(i)}) / B_i] \sin \phi_n^{(i)}, \\ \phi_{n+1}^{(i)} &= \phi_n^{(i)} - (\nu_i / \gamma_i) \ln |h_{n+1}^{(i)}|, \quad \text{mod } 2\pi, \\ \sigma_{n+1}^{(i)} &= \sigma_n^{(i)} \operatorname{sgn} h_{n+1}^{(i)}. \end{aligned} \quad (37)$$

It follows that the separatrix maps for the two systems are equivalent if

$$\begin{aligned} \nu_1 / \gamma_1 &= \nu_2 / \gamma_2, \\ M_1(+1) / M_1(-1) &= M_2(+1) / M_2(-1), \\ s_1 \epsilon_1 M_1 / B_1 &= s_2 \epsilon_2 M_2 / B_2. \end{aligned} \quad (38)$$

The first condition means that the perturbation frequency should be the same when measured in terms of the corresponding saddle-point eigenvalue γ_i . The second condition requires the ratio of Melnikov integrals for two separatrix branches to be the same for both systems, i.e., the perturba-

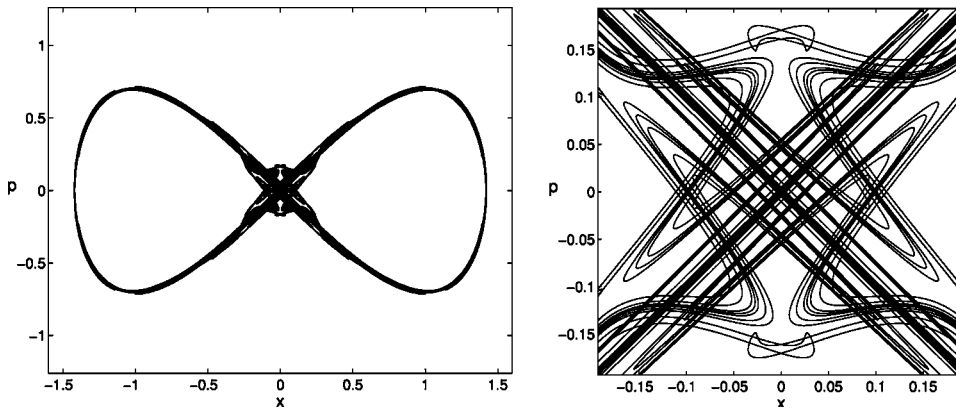


FIG. 3. Invariant manifolds for Duffing oscillator (41), $\epsilon_p = -0.0125 \dots$, $\nu_d = 4$ (a) Overview; (b) zoom of the saddle-point neighborhood.

functions $f_i(x, y)$ should have the same symmetry. The third condition relates the perturbation amplitudes, it can always be satisfied by setting

$$\epsilon_2 = \epsilon_1 \frac{s_1 M_1 B_2}{s_2 M_2 B_1}. \quad (39)$$

This equivalency of the separatrix maps is reflected in the structure of the homoclinic tangle: under the conditions (38) the phase portraits of $H^{(1)}$ and $H^{(2)}$ are similar to each other in the saddle-point neighborhood. The scaling factor follows from Eq. (36):

$$x_1 \rightarrow (B_2/B_1)^{1/2} x_2, \quad y_1 \rightarrow (B_2/B_1)^{1/2} y_2. \quad (40)$$

To verify the above universality, we numerically construct homoclinic tangles for two different systems, satisfying Eqs. (38). The first system is a Duffing oscillator with periodically modulated nonlinearity

$$H_\epsilon^d(p, x, t) = p^2/2 - x^2/2 + x^4/4a^2(1 + \epsilon_d \cos \nu_d t), \quad (41)$$

where ϵ_d and ν_d are the amplitude and the frequency of the modulation, and a is the parameter of the unperturbed potential. The second system is a parametrically perturbed pendulum with the Hamiltonian

$$H_\epsilon(p, x, t) = p^2/2 + (1 + \epsilon_p \cos \nu_p t) \cos x, \quad (42)$$

where ν_p and ϵ_p are the perturbation frequency and amplitude.

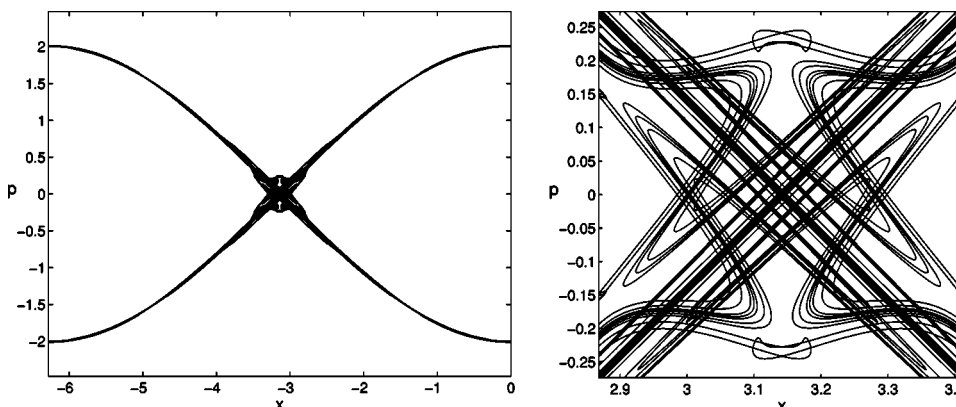


FIG. 4. Invariant manifolds of the pendulum (42) with the equivalent parameters [see, Eq. (46)]: $\nu_p = 4$, $\epsilon_p = -0.0416 \dots$ (a) Overview; (b) zoom of the saddle-point neighborhood. Axes are scaled according to Eq. (40) with respect to Fig. 3(b).

The asymptotics of the period of near-separatrix trajectories for Duffing oscillator is given by Eq. (5), which gives $B_d = 16a^2$. For the pendulum

$$T_p(E) \approx \ln 32/|E - E_s| \quad (43)$$

and $B_p = 32$.

The Melnikov integral for Eq. (41) is

$$M(\tau) = M_d \sin \nu \tau, \quad M_d = -\frac{\pi \nu^2 (\nu^2 + 4) a^2}{6 \sinh(\pi \nu/2)} \quad (44)$$

and for the pendulum

$$M(\tau) = M_p \sin \nu \tau, \quad M_p = \frac{2 \pi \nu^2}{\sinh(\pi \nu/2)}. \quad (45)$$

Note that the Duffing oscillator has $s_d = 1$ (phase space is a plane), but the pendulum has $s_p = -1$ (phase space is a cylinder).

The symmetry of the perturbation is the same in both systems: $M(+1) = M(-1)$, and the second condition in Eq. (38) is satisfied automatically. To satisfy the other two, we set

$$\nu_d = \nu_p, \quad \epsilon_d = \epsilon_p \frac{s_d M_p B_d}{s_p M_d B_p} = \epsilon_p 6 a^2 / (\nu^2 + 4). \quad (46)$$

We have numerically computed the stable and unstable invariant manifolds W^s and W^u attendant to the saddle point at the origin for both systems. The results are presented in Figs. 3 and 4. We have used the following parameter values

for the pendulum: $\epsilon_p = -0.0416 \dots$, $\nu_p = 4$. Corresponding values for the Duffing oscillator follow from Eq. (46): $\epsilon_d = -0.0125 \dots$, $\nu_d = 4$. Despite different forms of H_0 and V , and the difference in global topology of the phase space, the central parts of the two homoclinic tangles practically coincide when the axes are scaled according to Eq. (40).

V. CONCLUSION

Understanding the structure of the chaotic layer and its dependence on the parameters of the Hamiltonian is a key to many problems in physics, including cross-stream mixing in geophysical flows, orbital and spin-orbital resonances in celestial mechanics, destruction of magnetic surfaces in tokamaks, and many others. The width and the rough location of the layer are considered as the most important layer characteristics, but when the statistical properties of the particle motion are sought, the knowledge of its fine structure (the multifractal boundary) becomes essential. The connection to the anomalous particle statistics provides a motivation for studying the layer structure in detail.

Homoclinic tangle, formed by the broken separatrix, is a

backbone of the chaotic layer, its geometry determines transport properties of particles inside it. Due to the complexity of the tangle the problem of determination of fractal characteristics of the chaotic component (and of the resulting transport exponents) directly from the Hamiltonian remains largely an open question. The scaling similarity of the tangle demonstrated in this paper elucidates its dependence on the system's parameters and has important consequences for particle kinetics (such as $\ln \epsilon$ -periodic variation of the transport characteristics). The universality of the scaling, derived in Sec. IV, extends the invariance to different systems and allows to relate their statistical properties. The details of this relation will be discussed elsewhere.

ACKNOWLEDGMENTS

L.K. was supported by the Office of Naval Research under Grant No. N00014-93-1-0691. G.Z. was supported by the U.S. Navy Grants Nos. N00014-02-10056, N00014-97-1-0426, and the U.S. Department of Energy Grant No. DE-FG02-92ER54184.

-
- [1] H. Aref, *J. Fluid Mech.* **143**, 1 (1984).
 - [2] H. Aref, *Philos. Trans. R. Soc. London, Ser. A* **333**, 273 (1990).
 - [3] D. DelCastillo-Negrete, *Phys. Fluids* **10**, 576 (1998).
 - [4] J. Ottino, *The Kinematics of Mixing: Stretching, Chaos and Transport* (Cambridge University Press, Cambridge, 1989).
 - [5] K. Ngan and T. Shepherd, *J. Fluid Mech.* **334**, 315 (1997).
 - [6] J. Weiss and E. Knobloch, *Phys. Rev. A* **40**, 2579 (1989).
 - [7] G.M. Zaslavsky, *Fluid Dyn. Res.* **8**, 127 (1991).
 - [8] N.N. Filonenko and G.M. Zaslavsky [*Sov. Phys. JETP* **25**, 851 (1968)].
 - [9] A. Punjabi, A. Verma, and A. Boozer, *J. Plasma Phys.* **52**, 91 (1994).
 - [10] A. Iomin, D. Gangardt, and S. Fishman, *Phys. Rev. E* **57**, 4054 (1998).
 - [11] D. Rakhlin, *Phys. Rev. E* **63**, 011112 (2000).
 - [12] R. Malhotra, M. Holman, and T. Ito, *Proc. Natl. Acad. Sci. U.S.A.* **98**, 12342 (2001).
 - [13] I. Shevchenko, *Phys. Scr.* **57**, 185 (1998).
 - [14] C. Karney, *Physica D* **8**, 360 (1983).
 - [15] J. Hanson, J. Cary, and J. Meiss, *J. Stat. Phys.* **39**, 327 (1985).
 - [16] R. MacKay, J. Meiss, and I. Percival, *Physica D* **13**, 329 (1984).
 - [17] J. Meiss and E. Ott, *Physica D* **20**, 387 (1986).
 - [18] T.H. Solomon, E.R. Weeks, and H.L. Swinney, *Physica D* **76**, 70 (1994).
 - [19] V. Afraimovich and G. Zaslavsky, *Phys. Rev. E* **55**, 5418 (1997).
 - [20] L. Kuznetsov and G. Zaslavsky, *Phys. Rev. E* **61**, 3777 (2000).
 - [21] G. Zaslavsky, D. Stevens, and H. Weitzner, *Phys. Rev. E* **48**, 1683 (1993).
 - [22] G. Zaslavsky and M. Edelman, *Chaos* **10**, 135 (2000).
 - [23] V. Rom-Kedar, A. Leonard, and S. Wiggins, *J. Fluid Mech.* **214**, 347 (1990).
 - [24] V. Rom-Kedar and A. Poje, *Phys. Fluids* **11**, 2044 (1999).
 - [25] V. Rom-Kedar and G. Zaslavsky, *Chaos* **9**, 697 (1999).
 - [26] V. Melnikov, *Trans. Mosc. Math. Soc.* **12**, 1 (1963).
 - [27] B. Chirikov, *Phys. Rep.* **52**, 263 (1979).
 - [28] V. Rom-Kedar, *Nonlinearity* **7**, 441 (1994).
 - [29] D. Treschev, *Physica D* **116**, 21 (1998).
 - [30] G. Zaslavsky and S. Abdullaev, *Phys. Rev. E* **51**, 3901 (1995).
 - [31] S. Abdullaev and G. Zaslavsky, *Phys. Plasmas* **3**, 516 (1996).
 - [32] L. Kuznetsov and G. Zaslavsky, *Phys. Rep.* **288**, 457 (1997).
 - [33] S.S. Abdullaev and K. Spatschek, *Phys. Rev. E* **60**, 6287 (1999).
 - [34] S.S. Abdullaev, *Phys. Rev. E* **62**, 3508 (2000).
 - [35] J. Guckenheimer and P. Holmes, *Nonlinear Oscillations, Dynamical Systems, and Bifurcations of Vector Fields* (Springer-Verlag, New York, 1983).
 - [36] H. Nusse and J. Yorke, *Dynamics: Numerical Explorations* (Springer-Verlag, New York, 1998).
 - [37] R. McLachlan and P. Atela, *Nonlinearity* **5**, 541 (1991).
 - [38] G. Zaslavsky, R. Sagdeev, D. Usikov, and A. Chernikov, *Weak Chaos and Quasiregular Patterns* (Cambridge University Press, Cambridge, England, 1991).
 - [39] T. Ahn, G. Kim, and S. Kim, *Physica D* **89**, 315 (1996).
 - [40] S. Abdullaev and G. Zaslavsky, *Phys. Plasmas* **2**, 4533 (1995).
 - [41] I. Shevchenko, *J. Exp. Theor. Phys.* **91**, 615 (2000).
 - [42] A. Luo and R. Han, *Chaos, Solitons Fractals* **12**, 2493 (2001).
 - [43] A.J. Lichtenberg and M.A. Leiberman, *Regular and Chaotic Dynamics* (Springer-Verlag, New York, 1992).